Hypoxic and Ras-transformed cells support growth by scavenging unsaturated fatty acids from lysophospholipids

Jurre J. Kamphorst[a,b,1], Justin R. Cross[c,1], Jing Fan[a,b], Elisa de Stanchina[d], Robin Mathew[e,f], Eileen P. White[e,f,g], Craig B. Thompson[c,2], and Joshua D. Rabinowitz[a,b,e,2]

[a]Lewis-Sigler Institute for Integrative Genomics and [b]Department of Chemistry, Princeton University, Princeton, NJ 08544; [c]Cancer Biology and Genetics Program and [d]Antitumor Assessment Core Facility, Memorial Sloan Kettering Cancer Center, New York, NY 10065; [e]The Cancer Institute of New Jersey, New Brunswick, NJ 08903; [f]Robert Wood Johnson Medical School, University of Medicine and Dentistry of New Jersey, Piscataway, NJ 08854; and [g]Department of Molecular Biology and Biochemistry, Rutgers University, Piscataway, NJ 08854

Contributed by Craig B. Thompson, April 17, 2013 (sent for review February 22, 2013)

Cancer cell growth requires fatty acids to replicate cellular membranes. The kinase Akt is known to up-regulate fatty acid synthesis and desaturation, which is carried out by the oxygen-consuming enzyme stearoyl-CoA desaturase (SCD)1. We used ^{13}C tracers and lipidomics to probe fatty acid metabolism, including desaturation, as a function of oncogene expression and oxygen availability. During hypoxia, flux from glucose to acetyl-CoA decreases, and the fractional contribution of glutamine to fatty acid synthesis increases. In addition, we find that hypoxic cells bypass de novo lipogenesis, and thus, both the need for acetyl-CoA and the oxygen-dependent SCD1-reaction, by scavenging serum fatty acids. The preferred substrates for scavenging are phospholipids with one fatty acid tail (lysophospholipids). Hypoxic reprogramming of de novo lipogenesis can be reproduced in normoxic cells by Ras activation. This renders Ras-driven cells, both in culture and in allografts, resistant to SCD1 inhibition. Thus, a mechanism by which oncogenic Ras confers metabolic robustness is through lipid scavenging.

isotope tracing | lipogenesis in cancer | lipid metabolism

Cancer cells require a constant supply of energy and structural components to support their proliferation. Oncogenes actively reprogram metabolism to facilitate this supply (1, 2). Two of the most commonly activated pathways in human cancer are the PI3K-Akt and the Ras pathways (3). The metabolic effects of the PI3K-Akt pathway have been extensively studied, as, in addition to its role in cancer, this pathway is the primary effector of insulin signaling. Akt activation promotes glucose uptake, glycolytic flux, and lactate excretion, i.e., the Warburg effect (2). In addition, through downstream activation of mTOR, it increases protein synthesis (4). Finally, Akt induces lipogenesis through mechanisms including enzyme phosphorylation and transcriptional activation, like mTOR-dependent activation of SREBP1 (5, 6).

Fatty acids are a primary component of lipids. Their synthesis requires the generation of cytosolic acetyl-CoA (Fig. 1*A*). In normoxia, a predominant pathway involves catabolism of glucose to pyruvate, which is converted to mitochondrial acetyl-CoA by pyruvate dehydrogenase. Acetyl-CoA is then exported to the cytosol in the form of citrate, which is cleaved to generate cytosolic acetyl-CoA by ATP-citrate lyase, a direct Akt target. In hypoxia, pyruvate dehydrogenase is inactivated by pyruvate dehydrogenase kinase (7, 8), and glutamine-driven reductive carboxylation accounts for an increased fraction of citrate and thus acetyl-CoA (9–11).

Subsequent steps in the fatty acid synthesis pathway are catalyzed by acetyl-CoA carboxylase and fatty acid synthase, which are SREBP targets, and yield palmitate (C16:0, where 16 refers to the number of carbon atoms in the fatty acid, and 0 refers to the number of double bonds). Palmitate, in turn, is a substrate for various elongation and desaturation reactions to accommodate a cell's need for a diversity of fatty acids, of which the most abundant is the monounsaturated fatty acid oleate (C18:1) (12). Oleate is produced from palmitate by elongation to stearate (C18:0) followed by desaturation by Δ9 stearoyl-CoA desaturase (SCD)1, which requires oxygen as an electron acceptor. A specific ratio of oleate to stearate must be maintained by cells to ensure proper membrane fluidity and thus cell integrity, and a significant imbalance has been shown to induce apoptosis (13–15). SCD1 is regulated by the PI3K-Akt-mTOR pathway (5) and has been investigated as a pharmacological target for both obesity and cancer (16–19).

Like PI3K-Akt pathway activation, Ras activation induces glucose uptake and lactate excretion (20). Although Ras is known to activate the PI3K-Akt pathway, recent findings suggest that downstream metabolic effects may diverge. For example, Ras reduces mitochondrial respiration (21). In addition, Ras induces macropinocytosis and autophagy, thereby providing potential alternative sources of metabolic substrates (22–24). In further support of a divergent metabolic effect, mouse xenograft experiments revealed a difference in sensitivity to caloric restriction between Ras-driven tumors and tumors with PI3K-Akt activation (25). In contrast to the prolipogenic effect of Akt, the impact of Ras on lipid metabolism has not been investigated. Moreover, the interplay of oxygen availability and oncogene signaling on metabolism, including lipid metabolism, has not been extensively explored.

Here, we use ^{13}C tracers and lipidomics to study lipogenesis in transformed cells as a function of oncogene expression and oxygen availability. We find that hypoxia reduces the requirement for de novo fatty acid synthesis and desaturation by increasing fatty acid import. Oncogenic Ras recapitulates the hypoxic metabolic phenotype, and the increased reliance on fatty acid uptake renders Ras-driven cancer cells resistant to SCD1 inhibition. A major source of the imported fatty acids are serum lipids with one fatty acid tail, lysolipids. The ability to catabolize lipids with a single fatty acid tail was previously shown to be enhanced in aggressive and Ras-driven cancers (26–28). The present results show that related scavenging of lysolipids can be a major route of fatty acid acquisition in both hypoxia and Ras-driven cancer cells.

Results

Source of Cellular Fatty Acids Can Be Probed with ^{13}C-Labeled Glucose and Glutamine. Mammalian cells acquire fatty acids either through uptake or de novo synthesis (Fig. 1*A*). Fatty acid

Author contributions: J.J.K., J.R.C., J.F., E.d.S., E.P.W., C.B.T., and J.D.R. designed research; J.J.K., J.R.C., and J.F. performed research; R.M. contributed new reagents/analytic tools; J.J.K., J.R.C., and J.F. analyzed data; and J.J.K., J.R.C., C.B.T., and J.D.R. wrote the paper.

Conflict of interest statement: C.B.T. is a founder and consultant of Agios Pharmaceuticals and has a financial interest in Agios. C.B.T. is also on the Board of Directors of Merck.

[1]J.J.K. and J.R.C. contributed equally to this work.

[2]To whom correspondence may be addressed. E-mail: thompsonc@mskcc.org or joshr@genomics.princeton.edu.

This article contains supporting information online at www.pnas.org/lookup/suppl/doi:10.1073/pnas.1307237110/-/DCSupplemental.

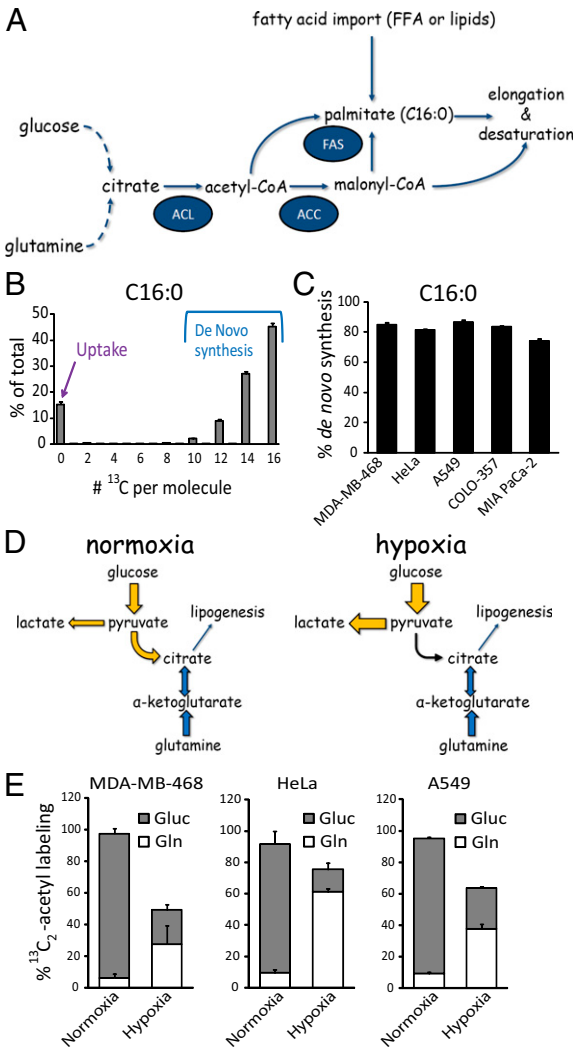

Fig. 1. Palmitate is mainly synthesized from glucose in normoxia, with increased fractional contribution from glutamine in hypoxia. (*A*) Schematic representation of de novo palmitate (C16:0) synthesis. ACC, acetyl-CoA carboxylase; ACL, ATP-citrate lyase; FAS, fatty acid synthase; FFA, free fatty acids. (*B*) Labeling pattern of palmitate (C16:0) saponified from cellular lipids, from MDA-MB-468 cells grown in [U-^{13}C]glucose and [U-^{13}C]glutamine for >five doublings. (*C*) Percentage of cellular palmitate (C16:0) fatty acid tails acquired through de novo synthesis, based on ^{13}C-labeling patterns as per *B*. (*D*) Schematic of the contribution of glucose and glutamine to lipogenesis in normoxia and hypoxia. (*E*) Percentage of labeling of acetyl groups from [U-^{13}C]glucose (Gluc) and [U-^{13}C]glutamine (Gln) in normoxia and hypoxia (1% O_2). Acetyl labeling from *N*-acetyl-glutamate and glutamate at steady state; analysis of fatty acid labeling gives equivalent results. All data are means ± SD of $n = 3$.

synthase makes the saturated fatty acid palmitate (C16:0), which can be desaturated and/or elongated to make a diversity of fatty acids. The metabolic routes to such fatty acids can be probed by supplying uniformly ^{13}C-labeled glucose and glutamine (to label acetyl-CoA) and subsequent mass spectrometry analysis of saponified fatty acids (29). For palmitate, such analysis at steady state labeling reveals an unlabeled fraction (M^0 peak) attributable to import of serum-derived fatty acids, as well as labeled forms arising from de novo lipogenesis. These labeled forms include [U-^{13}C]palmitate (M^{+16}) and partially labeled forms which arise because of incomplete acetyl-CoA labeling (Fig. 1*B*), with the relative abundance of the partially and fully labeled forms sufficient to determine the fractional labeling of cytosolic acetyl-CoA. Applying this approach to five cancer cell lines with diverse origins demonstrates that, in line with previous findings, in normoxic conditions, de novo lipogenesis accounts for 75–90% of the cellular C16:0 pool (Fig. 1*C*) (30).

In normoxia, glucose is the primary source for lipogenic acetyl-CoA. In contrast, in hypoxia (0.5–1% O_2), pyruvate dehydrogenase is less active. In such conditions, an increased fraction of citrate and thus acetyl-CoA is produced through glutamine-driven reductive carboxylation (Fig. 1*D*) (9–11). Consistent with this, when [U-^{13}C]glucose or [U-^{13}C]glutamine tracers are supplied separately, we find that glucose-derived carbon is the predominant acetyl-CoA source in normoxia, whereas glutamine-derived carbon contributes more in hypoxia (Fig. 1*E*).

Hypoxic Cells Bypass SCD1 by Importing Fatty Acids. The most abundant fatty acid in mammalian cells is oleate (C18:1), the main product of SCD1. The SCD1-catalyzed reaction is oxygen-dependent, and, therefore, we hypothesized that it might be slowed in hypoxia (Fig. 2*A*). To explore the effect of hypoxia on

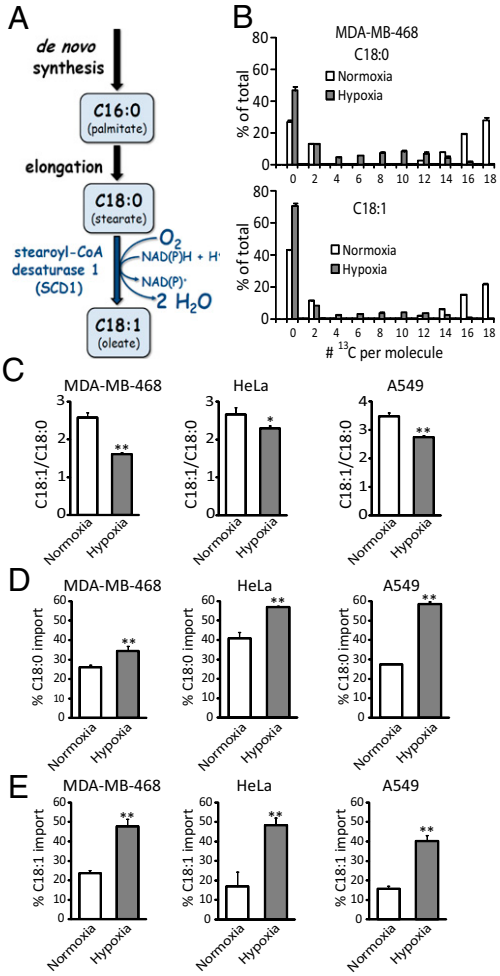

Fig. 2. Hypoxia decreases SCD1 flux and increases fatty acid import. (*A*) Schematic of oleate (C18:1) synthesis. (*B*) Labeling patterns of C18:0 and C18:1 from MDA-MB-468 cells grown in [U-^{13}C]glucose and [U-^{13}C]glutamine, in normoxia and hypoxia (1% O_2) for 72 h. (*C*) Desaturation index (C18:1/C18:0) in normoxia and hypoxia (1% O_2 for MDA-MB-468 and HeLa cells and 0.5% for A549 cells). (*D* and *E*) Percentage of import of C18:0 (*D*) and C18:1 (*E*) pools in normoxia and hypoxia, as measured by fatty acid labeling for 72 h, from [U-^{13}C]glucose and [U-^{13}C]glutamine. All data are means ± SD of $n = 3$. *$P < 0.05$; **$P < 0.01$ (two-tailed *t* test).

fatty acid synthesis, elongation, and desaturation, we simultaneously fed [U-^{13}C]glucose and [U-^{13}C]glutamine to hypoxic cells and observed that fatty acid labeling was decreased compared with normoxia, with increased unlabeled (M^0) peaks indicative of enhanced fatty acid import from serum (Fig. 2*B* and Fig. S1). Consistent with impaired SCD1 activity, the decrease in labeling was particularly profound for the monounsaturated fatty acid C18:1 (Fig. 2*B* and Fig. S1). This decreased C18:1 labeling is also associated with an overall change in cellular lipid composition, in the direction of saturated fatty acids (lower C18:1/C18:0 ratio, or "desaturation index"; Fig. 2*C*). Thus, cellular lipid composition per se is impacted by hypoxia, indicating that import is insufficient to fully compensate for the impaired SCD1 activity.

In cells fed [U-^{13}C]glucose and [U-^{13}C]glutamine, C16:0 elongation to C18:0 usually adds labeled carbon. Thus, the only major route to unlabeled C18:0, which is modestly increased in hypoxia (Fig. 2*D*), is import from serum. In contrast, in addition to direct uptake, unlabeled C18:1 can arise from desaturation of unlabeled C18:0 (Fig. 2*A*). To confirm that SCD1 activity is decreased in hypoxia, we use the labeling data (where L_{cell} equals the fraction of a given cellular fatty acid that is labeled) to calculate *D,* the fraction of C18:1 made by SCD1. Fractional import *I* equals 1 – *D*. Because serum fatty acids are not labeled, the only route to labeled C18:1 is desaturation of labeled C18:0:

$$L_{cell\ C18:1} = (D)(L_{cell\ C18:0}) \quad [1]$$

$$D = L_{cell\ C18:1}/L_{cell\ C18:0} \quad [2]$$

We find that *D* is indeed decreased, and, thus C18:1 import increased, in hypoxia (Fig. 2*E*).

Oncogenic Ras Recapitulates Hypoxic Metabolism. In addition to the effects of hypoxia, we examined the contribution of specific oncogenes to the balance between de novo lipogenesis and fatty acid import. Like hypoxia, oncogenic Akt and Ras have been implicated in increasing glucose uptake in transformed cells (3, 20). Whereas the PI3K-Akt pathway has been shown to promote lipogenesis, the impact of Ras on fatty acid metabolism has not been well studied. We, therefore, examined fatty acid metabolism in an isogenic cellular model system: immortalized baby mouse kidney (iBMK) cells with no oncogene (CTL); membrane-targeted and, thus, activated Akt (myrAkt); or oncogenic H-Ras (H-Ras^{V12G}) (31, 32). Introduction of myrAkt resulted in increased de novo synthesis of monounsaturated (but not saturated) fatty acids, as evidenced by an increased desaturation index (C18:1/C18:0) and decrease in the fraction of monounsaturated fatty acids coming from import (Fig. 3 *A* and *B* and Fig. S2). In contrast, oncogenic H-Ras^{V12G} caused a decrease in the desaturation index, indicating that Ras and Akt activation lead to fundamentally different cellular lipid composition. In addition, oncogenic H-Ras^{V12G} increased the fraction of cellular fatty acids acquired via import. This was most pronounced for C18:1, implying reduced SCD1 flux. The increased utilization of serum-derived fatty acids by Ras-driven cells was confirmed by direct measurements of fatty acid uptake from medium (Fig. 3*C*).

To examine the generality of the impact of oncogenic Ras on monounsaturated fatty acid uptake, we used human pancreatic nestin-expressing (HPNE) cells with no oncogene (CTL) or oncogenic K-Ras (K-Ras^{G12D}). Like oncogenic H-Ras^{V12G} in iBMK cells, expression of oncogenic K-Ras^{G12D} in HPNE cells led to a lower desaturation index, more incorporation of serum C18:1 into cellular lipids, and faster serum C18:1 uptake (Fig. 3 *D–F*).

We next examined the impact of Ras versus Akt on other metabolic parameters impacted by hypoxia: glucose uptake, lactate excretion, oxygen consumption, and glutamine metabolism. In iBMK cells, both oncogenic Ras and Akt caused an increase in glucose uptake and increased shunting of glucose-derived carbon toward lactate (Fig. 3*G*). However, whereas Akt-transformed cells maintained oxygen consumption at levels comparable to control cells, Ras-transformed cells displayed a significant decrease in oxygen consumption and increased fractional contribution of reductive carboxylation flux to citrate synthesis, as evidenced by increased $^{13}C_5$-labeled citrate in cells fed [U-^{13}C]glutamine (Fig. 3 *H* and *I*) (33). Similar results were observed in K-Ras^{G12D} transformed HPNE cells (Fig. 3 *J–L*). Taken together, these results demonstrate that oncogenic Ras has an opposite effect to Akt with respect to regulation of fatty acid metabolism in general and SCD1 flux, in particular, and that it recapitulates a metabolic phenotype of hypoxic cells.

Oncogenic Ras Confers Resistance to SCD1 Inhibition. SCD1 inhibition can block the growth of cancer cells, both in vitro and in xenografts (17, 19). In experiments with A549 lung cancer cells, however, an SCD1 inhibitor dose (200 nM CAY10566) that completely blocked C18:1 labeling (Fig. 4*A*), did not impair cell growth in a real-time cell proliferation assay (10% serum; Fig. 4*B*) or for the first 48 h of growth in standard cell culture conditions (Fig. S3). Consistent with the persistent cell growth being supported by serum lipids, switching to 2% serum rendered the cells sensitive to SCD1 inhibition (Fig. 4*B*). Because A549 cells naturally express oncogenic K-Ras (34), and Ras promotes C18:1 uptake, we hypothesized that constitutive Ras activation might induce resistance to SCD1 inhibition. To explore this, we grew

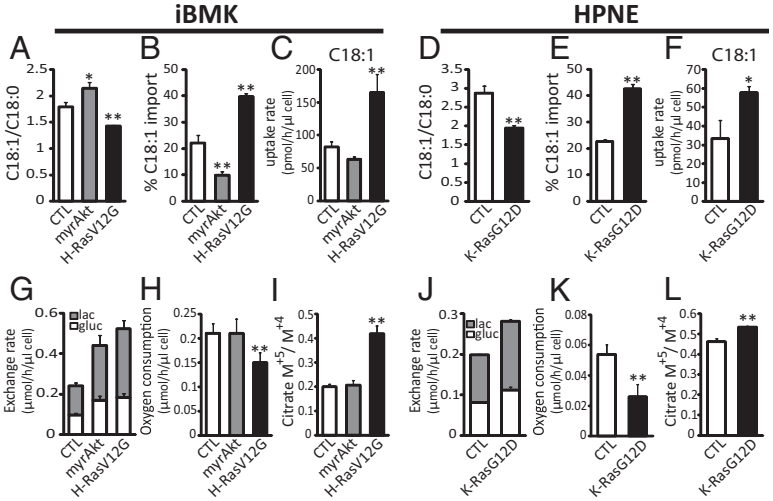

Fig. 3. Oncogenic Ras mimics hypoxia, increasing fatty acid scavenging and acetyl-CoA labeling from glutamine and decreasing oxygen consumption. (*A*) Desaturation index (C18:1/C18:0) in iBMK isogenic cell lines engineered to express myrAkt or H-Ras^{V12G} versus vector control (CTL). (*B*) Percentage of import of C18:1, as measured by steady-state fatty acid labeling from [U-^{13}C]glucose and [U-^{13}C]glutamine. (*C*) Uptake rates of C18:1, based on measurements of saponified lipids from fresh and spent medium (10% serum; 72 h of incubation). (*D–F*) Same measurements for HPNE cells with oncogenic K-Ras^{G12D} versus vector control (CTL). (*G*) Glucose uptake and lactate excretion in iBMK cells. gluc, glucose; lac, lactate. (*H*) Oxygen consumption. (*I*) Ratio of citrate produced from reductive carboxylation of glutamine-derived α-ketoglutarate (M^{+5}) to oxidative metabolism (M^{+4}). (*J–L*) Same measurements in HPNE cells. All data are means ± SD of $n \geq 3$. *$P < 0.05$; **$P < 0.01$ (two-tailed *t* test).

iBMK cells with H-Ras^{V12G} or myrAkt in the presence of SCD1 inhibitor. The inhibitor fully blocked SCD1 in both cell lines (Fig. S4). Nevertheless, in 10% serum, whereas growth of myrAkt cells was severely impaired, the H-Ras^{V12G} cells grew almost normally for three population doublings (Fig. 4*C* and Fig. S3).

To determine robustness against SCD1 inhibition in vivo, athymic nude mice were injected with iBMK cells with myrAkt or H-Ras^{V12G}. After establishment of palpable tumors, the mice were treated with vehicle or SCD1 inhibitor (2.5 mg/kg CAY10566 orally twice daily). The effect of SCD1 inhibition on the Akt-driven tumors was greater than on the Ras-driven tumors (Fig. 4 *D* and *E*), with the mean tumor volume at day 13 or 14 post therapy, relative to untreated tumors, $0.51^{+/-}$ 0.04 and $0.67^{+/-}$ 0.05 respectively ($P = 0.01$ for Ras-Akt comparison, by two-tailed t test). Thus, oncogenic Ras (at least relative to activated Akt) confers resistance to SCD1 inhibition, both in vitro and in allografts.

Imported Fatty Acids Originate from Lysophospholipids. The above results demonstrate that oncogenic Ras increases import of exogenous fatty acids, conferring resistance against SCD1 inhibition. Although free (nonesterified) fatty acids have been shown to rescue cell proliferation during SCD1 inhibition when supplemented in large enough quantities (13, 17), their levels in serum are insufficient to account for the observed fatty acid uptake and associated cell growth (Table S1).

To identify which lipids were the source for the scavenged fatty acids, we profiled glycerophospholipid levels by mass spectrometry in fresh and spent medium (Fig. 5*A*). The levels of typical glycerophospholipids (i.e., glycerol with a head group and two fatty acid tails) did not change substantially. However, we observed a near total depletion of the glycerophospholipids with only one fatty acid tail (lysophospholipids; Fig. 5*B*). The selective lysophospholipid depletion was observed for all cell lines tested (Fig. S5*A*).

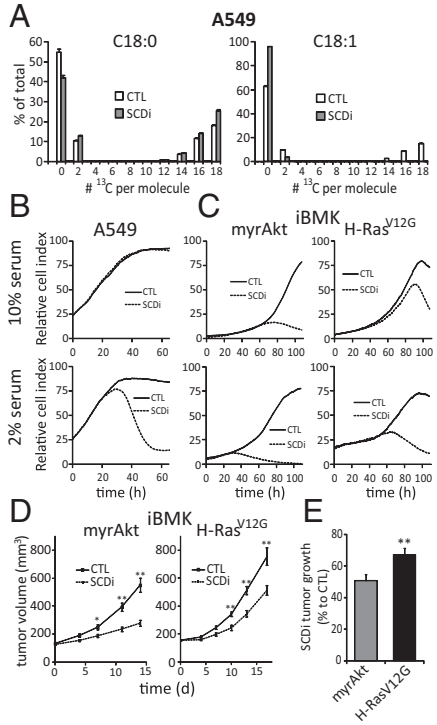

Fig. 4. Differential impact of Ras and Akt on sensitivity to SCD1 inhibition. (*A*) CAY10566 (200 nM) [SCD1 inhibitor (SCDi)] blocks C18:1 labeling from [U-^{13}C]glucose and [U-^{13}C]glutamine. (*B* and *C*) Impact of SCDi on A549, iBMK–H-Ras^{V12G}, and iBMK-myrAkt cell growth in xCELLigence instrument. CTL is vehicle control. (*D*) Growth of allografted iBMK–H-Ras^{V12G} and iBMK-myrAkt tumors treated with vehicle (CTL) or SCDi (CAY10566, 2.5 mg/kg orally twice daily). (*E*) Percentage of growth of iBMK–H-Ras^{V12G} and iBMK-myrAkt tumors relative to untreated controls, after 13 and 14 d treatment with SCDi, respectively. For *A*–*C*, data are means ± SD of $n \geq 3$. For *D* and *E*, data are means ± SEM of $n = 10$ mice per group. *$P < 0.05$; **$P < 0.01$ (two-tailed t test).

Lysolipids Support Growth of Ras-Driven Cells. Quantitative analysis of lysolipid uptake suggests that lysophosphatidylcholine (LPC) (18:1) plays a significant role in meeting cellular demand for monounsaturated fatty acids: in iBMK–H-Ras^{V12G} cells treated with SCD1 inhibitor, the uptake of LPC(18:1) over 48 h was comparable to the total cellular C18:1 incorporation during this time period (Fig. 3*C* and Figs. S3 and S5), and depletion of serum LPC(18:1) occurred simultaneous with growth inhibition (Figs. S3 and S5).

To further evaluate LPC(18:1) as a nutrient, we spiked the medium of the iBMK cells with 20 μM LPC(18:1), half the concentration found in 100% serum (i.e., physiological conditions) (35). The desaturation index (C18:1/C18:0), initially more than twofold higher in iBMK-myrAkt cells than iBMK–H-Ras^{V12G} cells, increased significantly and selectively in iBMK–H-Ras^{V12G} cells upon addition of LPC(18:1) (Fig. 5*C*). This coincided with the fraction of C18:1 derived from import, although increasing for both cell lines with LPC(18:1) addition, being more than twice as high in iBMK–H-Ras^{V12G} cells (Fig. 5*D*). Consistent with a differential dependency on SCD1 relative to C18:1 import, LPC (18:1) supplementation during SCD1 inhibition fully restored proliferation for iBMK–H-Ras^{V12G} cells but only partially for iBMK-myrAkt cells (Fig. 5 *E* and *F*). Similarly, a complete rescue was observed for the Ras-driven A549 human cancer cell line (Fig. 5*G*).

The analysis of serum lipid consumption suggested that lysolipids provide a more accessible nutrient source than serum glycerophospholipids. Consistent with this, in SCD1 inhibitor-treated cells, supplementation with phosphatidylcholine (PC)(16:0,18:1) did not restore cell growth (Fig. 5*E*). A possible explanation is the presence also of the saturated tail (C16:0). Indeed, supplementation with saturated lysolipid LPC(18:0) caused stronger growth inhibition than SCD1 inhibition alone. However, simultaneous incubation with LPC(18:1) and LPC(18:0) restored growth, proving that the growth restoration with LPC(18:1) but not PC(16:0,18:1) reflects greater cellular access to the lysolipid's monounsaturated fatty acid tail. Consistent with lysolipids being preferred substrates for fatty acid scavenging, oleoyl-monoacylglycerol [MG(18:1)], also restored cell proliferation. Thus, lysolipid scavenging can meet cellular monounsaturated fatty acid needs.

Discussion

Tumors require fatty acids to replicate their cellular membranes and thereby grow. It is commonly assumed that cancer cells synthesize most of their nonessential fatty acids de novo. This assumption is based primarily on cell culture experiments conducted in 10% serum and normoxia. It is supported by the glucose-dependent prolipogenic effects of one of the most important oncogenic pathways, PI3K-Akt-mTOR. Because Ras activates Akt (3, 36), Ras might also have a glucose-dependent prolipogenic role.

In contrast, here we find that Ras does not induce glucose-dependent de novo lipogenesis but, instead, stimulates scavenging of serum fatty acids. Such scavenging is an intrinsic property of all cells we studied and is further increased by Ras activation, hypoxia, and addition to media of physiological concentrations of lysophospholipid (i.e., phospholipids with only one fatty acid tail). Enhanced scavenging renders Ras-driven cells resistant to pharmacological inhibition of the main mammalian desaturase, SCD1. Moreover, it may facilitate the growth of Ras-driven tumors in hypoxic conditions by circumventing SCD1, which requires molecular oxygen as an electron acceptor.

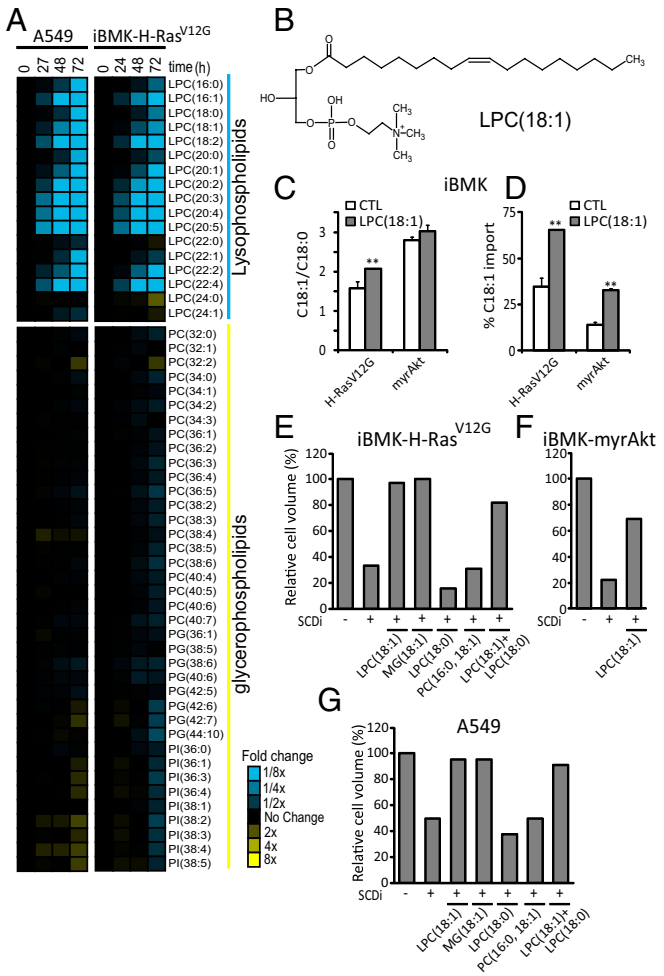

Fig. 5. Fatty acids are scavenged from lysophospholipids. (*A*) Fold changes in medium phospholipids during growth of A549 and iBMK–H-Ras^{V12G} cells (relative to fresh medium with 10% serum). (*B*) Structure of LPC(18:1). (*C*) Effect of LPC(18:1) supplementation (20 μM; 72 h) on desaturation index (C18:1/C18:0). (*D*) Percentage of contribution of import to the cellular C18:1 pool based on [U-^{13}C]glucose and [U-^{13}C]glutamine labeling in iBMK–H-Ras^{V12G} and iBMK-myrAkt cells. (*E*–*G*) Packed cell volume for iBMK–H-Ras^{V12G} (*E*), iBMK-myrAkt (*F*), and A549 (*G*) cells [relative to untreated control (CTL)] after 72 h of incubation with or without 200 nM SCDi (CAY10566), in the presence of the indicated supplemented lipids (20 μM). PG, phosphatidylglycerol; PI, phosphatidylinositol. Data are mean $n = 3$ (*A*); means ± SD of $n = 3$ (*C* and *D*), and mean $n = 2$ (*E*–*G*). *$P < 0.05$; **$P < 0.01$ (two-tailed t test).

Both Ras activation and hypoxia, in addition to inducing fatty acid scavenging, also increase the fraction of acetyl-CoA units produced from glutamine. Moreover, Ras activation leads to decreased oxygen consumption. What is the source of the metabolic parallels between hypoxia and Ras activation? One possibility is that both Ras and hypoxia activate hypoxia-inducible factor (HIF) (or both converge on another signaling protein) (37), which, in turn, produces the observed metabolic commonalities. Another is that Ras activation, like hypoxia, directly impairs oxidative phosphorylation, leading to increased NADH (or another metabolite), which, in turn, leads to the lipid metabolic changes. In support of this latter possibility, Ras has recently been shown to migrate to the mitochondrion and inhibit complex I (21).

The key substrates of the fatty acid scavenging pathway are serum lysophospholipids. In contrast to standard phospholipids with two tails, lysophospholipids provide a readily accessible fatty acid source for cells. For example, oleoyl-LPC, but not a corresponding PC species with two fatty acid tails, rescues cells from SCD1 inhibition. Although free oleate (C18:1) can also rescue cells from SCD1 inhibition, lysophospholipids are more abundant than free fatty acids in serum and, thus, likely a more important physiological source. For example, about 20% of serum oleate is in the form of oleoyl-LPC compared with 5% in the free fatty acid form.

The mechanism by which cells scavenge lysophospholipids remains to be elucidated. Important questions include the mechanisms of lipid import and subsequent metabolism. Intriguingly, the enzyme MG lipase (MAGL), which generates free fatty acids from monoacylglycerols, is highly expressed in aggressive cancer cells and its over-expression enhances tumorigenicity (26). Its expression is also increased by the H-Ras and the K-Ras–HIF pathways (27, 28). Although it has been previously hypothesized that the relevance of MAGL to cancer is via enhancing the levels of protumorigenic lipid messengers such as lysophosphatidic acid and PGE_2, it may also contribute to lysolipid scavenging.

The uptake and utilization of lysophospholipids by Ras-driven cells is part of a more global "scavenger" metabolic phenotype. Oncogenic Ras up-regulates both autophagy and macropinocytosis, both involving uptake of bulk material into endocytotic vesicles (22–24). The former consumes intracellular contents (cellular cannibalism) and the latter extracellular ones. Both can provide nutrition via macromolecule degradation, and it is possible that macropinocytosis contributes directly to lysolipid uptake.

Irrespective of a potential role for macropinocytosis, scavenging is a metabolic hallmark of Ras-driven cancers. Whereas tumors driven by the PI3K-Akt pathway wantonly engage in biosynthesis and become metabolically vulnerable (38), those driven primarily by oncogenic Ras instead have the capacity to maintain rapid growth by using extracellular macromolecules to obtain the required substrates for new macromolecule and lipid production. This has therapeutic implications, rendering Ras-driven tumors comparatively robust to inhibitors of anabolic enzymes such as SCD1. At the same time, it raises hope that scavenging pathway enzymes may be therapeutic targets for Ras-driven cancers. Clear definition of the molecular steps of scavenging pathways will lay the groundwork for testing this exciting possibility.

Experimental Procedures

Cell Culturing, SCD1 Inhibition, and Lipid Supplementation. Cell lines were from ATCC with the following exceptions: the iBMK cell lines were derived from primary kidney epithelial cells from Bax$^{-/-}$/Bak$^{-/-}$ mice, immortalized by E1A and dominant-negative p53 expression, and transfected with control vector, human oncogenic H-Ras^{V12G}, or myrAkt (31); and HPNE cells (a generous gift of A. Maitra, Johns Hopkins University, Baltimore) were developed from human pancreatic duct by transduction with a retroviral expression vector (pBABEpuro) containing the hTERT gene and transfected with control vector or human oncogenic K-Ras^{G12D}. Cell lines were routinely passaged in Dulbecco's modified Eagle medium (DMEM) (Mediatech) with 25 mM glucose and 4 mM glutamine and supplemented with 10% (vol/vol) FBS (HyClone), 25 IU/mL penicillin, and 25 μg/mL streptomycin (MP Biomedicals) and split at 80% confluence. Metabolic experiments were performed in 6-cm culture dishes with 3 mL of DMEM containing 10% dialyzed FBS (HyClone). For isotope labeling, glucose and glutamine were replaced with their U-^{13}C–labeled forms (Cambridge Isotope Laboratories). Hypoxia experiments were performed in a hypoxic glove box (0.5% or 1% O_2 as indicated, 5% CO_2 and 94–94.5% N_2; 37 °C) (Coy Laboratory Products). Cells and media were equilibrated in low oxygen overnight before experiment initiation. CAY10566 was from Cayman Chemical. Lipid supplements were from Avanti Polar Lipids. LPC(18:1) and LPC(18:0) were dissolved in PBS; MG(18:1) was dissolved in methanol; and PC(16:0 to 18:1) was dissolved in 1:9 chloroform: methanol. Organic solvents were <0.1% vol/vol in the medium.

Cell Proliferation Assays and Tumor Xenograft Studies. Cell proliferation was determined with either packed cell volume tubes (Techno Plastic Products) or with the xCELLigence system (Roche). Animal studies were performed following the guidelines for proper and humane use of animals in research under an Institutional Animal Care and Use Committee-approved protocol at Memorial Sloan-Kettering Cancer Center. To generate allografts, 1×10^7

iBMK cells were implanted in Matrigel (BD Biosciences) into nu/nu athymic female mice. After establishment of palpable tumors, mice were randomized to receive 2.5 mg/kg CAY10566 orally twice daily in 0.5% methylcellulose or vehicle control. Xenograft tumors were measured biweekly and tumor volume calculated as volume = (length × width^2 × π)/6.

Lipid and Metabolite Measurements. For saponified fatty acid analysis from cells, media were aspirated, cells were rinsed twice with 2 mL of room temperature PBS, 1 mL of 50:50 MeOH/H_2O solution with 0.1 M HCl at –20 °C was added, and the resulting liquid and cell debris scraped into a microfuge tube. For analogous measurements from media, 0.5 mL of medium was mixed with 0.5 mL of MeOH with 0.2 M HCl. Chloroform (0.5 mL) was added, the mixture was vortexed for 1 min and then centrifuged at 16,000 × *g* for 5 min, and the chloroform layer was transferred to a glass vial. The extract was dried under N_2, reconstituted into 90:10 MeOH/H_2O containing 0.3 M KOH, incubated at 80 °C for 1 h to saponify fatty acids, acidified with 0.1 mL of formic acid, extracted twice with 1 mL of hexane, dried under N_2, and reconstituted into 1:1:0.3 MeOH:chloroform:H_2O (1 mL of solvent per 2 μL of packed volume for cells, and 2 mL of solvent total for the medium samples) for liquid chromatography–mass spectrometry (LC-MS) analysis. Separation was by reversed-phase ion-pairing chromatography on a C8 column coupled to negative-ion mode, full-scan LC-MS at 1-Hz scan time and 100,000 resolving power (stand-alone orbitrap; Thermo Fischer Scientific) (29).

For analysis of lipids in culture medium, the dried chloroform extract from 0.5 mL medium was obtained as above, reconstituted in 0.3 mL 1:1:0.3 MeOH:chloroform:H_2O and analyzed by LC-MS as above. For analysis of free (nonesterified) fatty acids, 1 mL medium was extracted three times with 1 mL ethyl acetate and the extract dried and reconstituted in 0.5 mL 1:1:0.3 MeOH:chloroform:H_2O. For analysis of water soluble metabolites, media was aspirated from the cells and metabolism quenched immediately with 80:20 MeOH/H_2O at –80ºC. The resulting liquid and cell debris were then scraped into a microfuge tube and extracted three times with 80:20 MeOH at –80 °C, and the extract was dried under N_2, reconstituted into H_2O (50 μL/μL cell volume), and analyzed by LC-MS as above except using a C18 column (39). Medium glucose and lactate concentrations were measured with an YSI7200 electrochemical analyzer (YSI). Oxygen consumption was determined using a Seahorse XF24 flux analyzer (Seahorse Bioscience).

ACKNOWLEDGMENTS. This work was supported by National Institutes of Health Grants P50GM071508 and 1R01CA16359-01A1 and by Stand Up To Cancer. J.J.K. is a Hope Funds for Cancer Research Fellow (HFCR-11-03-01). J.F. is a Howard Hughes Medical Institute International Student Research Fellow.

1. Deberardinis RJ, Sayed N, Ditsworth D, Thompson CB (2008) Brick by brick: Metabolism and tumor cell growth. *Curr Opin Genet Dev* 18(1):54–61.
2. Vander Heiden MG, Cantley LC, Thompson CB (2009) Understanding the Warburg effect: The metabolic requirements of cell proliferation. *Science* 324(5930):1029–1033.
3. Shaw RJ, Cantley LC (2006) Ras, PI(3)K and mTOR signalling controls tumour cell growth. *Nature* 441(7092):424–430.
4. Gingras A-C, Raught B, Sonenberg N (2001) Regulation of translation initiation by FRAP/mTOR. *Genes Dev* 15(7):807–826.
5. Luyimbazi D, et al. (2010) Rapamycin regulates stearoyl CoA desaturase 1 expression in breast cancer. *Mol Cancer Ther* 9(10):2770–2784.
6. Menendez JA, Lupu R (2007) Fatty acid synthase and the lipogenic phenotype in cancer pathogenesis. *Nat Rev Cancer* 7(10):763–777.
7. Kim J-W, Tchernyshyov I, Semenza GL, Dang CV (2006) HIF-1-mediated expression of pyruvate dehydrogenase kinase: A metabolic switch required for cellular adaptation to hypoxia. *Cell Metab* 3(3):177–185.
8. Papandreou I, Cairns RA, Fontana L, Lim AL, Denko NC (2006) HIF-1 mediates adaptation to hypoxia by actively downregulating mitochondrial oxygen consumption. *Cell Metab* 3(3):187–197.
9. Metallo CM, et al. (2012) Reductive glutamine metabolism by IDH1 mediates lipogenesis under hypoxia. *Nature* 481(7381):380–384.
10. Wise DR, et al. (2011) Hypoxia promotes isocitrate dehydrogenase-dependent carboxylation of α-ketoglutarate to citrate to support cell growth and viability. *Proc Natl Acad Sci USA* 108(49):19611–19616.
11. Mullen AR, et al. (2012) Reductive carboxylation supports growth in tumour cells with defective mitochondria. *Nature* 481(7381):385–388.
12. Guillou H, Zadravec D, Martin PGP, Jacobsson A (2010) The key roles of elongases and desaturases in mammalian fatty acid metabolism: Insights from transgenic mice. *Prog Lipid Res* 49(2):186–199.
13. Hess D, Chisholm JW, Igal RA (2010) Inhibition of stearoylCoA desaturase activity blocks cell cycle progression and induces programmed cell death in lung cancer cells. *PLoS ONE* 5(6):e11394.
14. Green CD, Olson LK (2011) Modulation of palmitate-induced endoplasmic reticulum stress and apoptosis in pancreatic β-cells by stearoyl-CoA desaturase and Elovl6. *Am J Physiol Endocrinol Metab* 300(4):E640–E649.
15. Hardy S, Langelier Y, Prentki M (2000) Oleate activates phosphatidylinositol 3-kinase and promotes proliferation and reduces apoptosis of MDA-MB-231 breast cancer cells, whereas palmitate has opposite effects. *Cancer Res* 60(22):6353–6358.
16. Miyazaki M, et al. (2009) Stearoyl-CoA desaturase-1 deficiency attenuates obesity and insulin resistance in leptin-resistant obese mice. *Biochem Biophys Res Commun* 380(4):818–822.
17. Roongta UV, et al. (2011) Cancer cell dependence on unsaturated fatty acids implicates stearoyl-CoA desaturase as a target for cancer therapy. *Mol Cancer Res* 9(11):1551–1561.
18. Igal AR (2011) Roles of stearoylCoA desaturase-1 in the regulation of cancer cell growth, survival and tumorigenesis. *Cancers* 3(2):2462–2477.
19. Mason P, et al. (2012) SCD1 inhibition causes cancer cell death by depleting monounsaturated fatty acids. *PLoS ONE* 7(3):e33823.
20. Ying H, et al. (2012) Oncogenic Kras maintains pancreatic tumors through regulation of anabolic glucose metabolism. *Cell* 149(3):656–670.
21. Hu Y, et al. (2012) K-ras^{G12V} transformation leads to mitochondrial dysfunction and a metabolic switch from oxidative phosphorylation to glycolysis. *Cell Res* 22(2):399–412.
22. Guo JY, et al. (2011) Activated Ras requires autophagy to maintain oxidative metabolism and tumorigenesis. *Genes Dev* 25(5):460–470.
23. Yang S, et al. (2011) Pancreatic cancers require autophagy for tumor growth. *Genes Dev* 25(7):717–729.
24. Bar-Sagi D, Feramisco JR (1986) Induction of membrane ruffling and fluid-phase pinocytosis in quiescent fibroblasts by ras proteins. *Science* 233(4768):1061–1068.
25. Kalaany NY, Sabatini DM (2009) Tumours with PI3K activation are resistant to dietary restriction. *Nature* 458(7239):725–731.
26. Nomura DK, et al. (2010) Monoacylglycerol lipase regulates a fatty acid network that promotes cancer pathogenesis. *Cell* 140(1):49–61.
27. Chun SY, et al. (2010) Oncogenic KRAS modulates mitochondrial metabolism in human colon cancer cells by inducing HIF-1α and HIF-2α target genes. *Mol Cancer* 9:293.
28. Joyce T, Cantarella D, Isella C, Medico E, Pintzas A (2009) A molecular signature for epithelial to mesenchymal transition in a human colon cancer cell system is revealed by large-scale microarray analysis. *Clin Exp Metastasis* 26(6):569–587.
29. Kamphorst JJ, Fan J, Lu W, White E, Rabinowitz JD (2011) Liquid chromatography-high resolution mass spectrometry analysis of fatty acid metabolism. *Anal Chem* 83(23):9114–9122.
30. Kannan R, Lyon I, Baker N (1980) Dietary control of lipogenesis in vivo in host tissues and tumors of mice bearing Ehrlich ascites carcinoma. *Cancer Res* 40(12):4606–4611.
31. Degenhardt K, White E (2006) A mouse model system to genetically dissect the molecular mechanisms regulating tumorigenesis. *Clin Cancer Res* 12(18):5298–5304.
32. Degenhardt K, Chen G, Lindsten T, White E (2002) BAX and BAK mediate p53-independent suppression of tumorigenesis. *Cancer Cell* 2(3):193–203.
33. Gaglio D, et al. (2011) Oncogenic K-Ras decouples glucose and glutamine metabolism to support cancer cell growth. *Mol Syst Biol* 7:523.
34. Krypuy M, Newnham GM, Thomas DM, Conron M, Dobrovic A (2006) High resolution melting analysis for the rapid and sensitive detection of mutations in clinical samples: KRAS codon 12 and 13 mutations in non-small cell lung cancer. *BMC Cancer* 6:295.
35. Sasagawa T, Okita M, Murakami J, Kato T, Watanabe A (1999) Abnormal serum lysophospholipids in multiple myeloma patients. *Lipids* 34(1):17–21.
36. Khwaja A, Rodriguez-Viciana P, Wennström S, Warne PH, Downward J (1997) Matrix adhesion and Ras transformation both activate a phosphoinositide 3-OH kinase and protein kinase B/Akt cellular survival pathway. *EMBO J* 16(10):2783–2793.
37. Sheta EA, Trout H, Gildea JJ, Harding MA, Theodorescu D (2001) Cell density mediated pericellular hypoxia leads to induction of HIF-1alpha via nitric oxide and Ras/MAP kinase mediated signaling pathways. *Oncogene* 20(52):7624–7634.
38. Schulze A, Harris AL (2012) How cancer metabolism is tuned for proliferation and vulnerable to disruption. *Nature* 491(7424):364–373.
39. Lu W, et al. (2010) Metabolomic analysis via reversed-phase ion-pairing liquid chromatography coupled to a stand alone orbitrap mass spectrometer. *Anal Chem* 82(8):3212–3221.